A

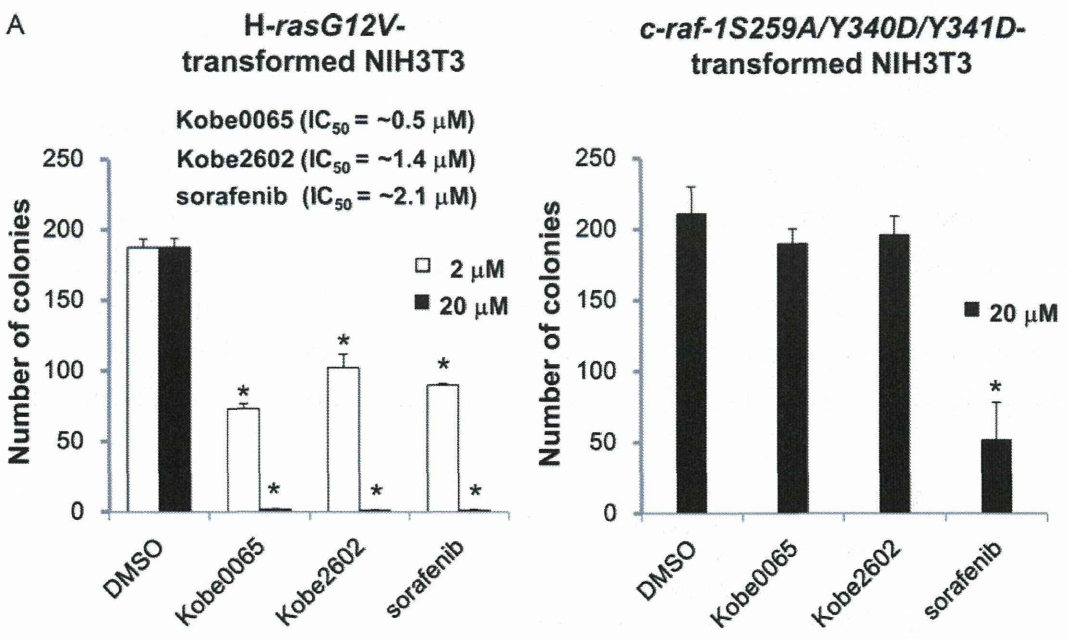


B

| Cell line | Organ | Ras | B-Raf | PTEN | PIK3CA | Inhibitory effect (%) | | |
|---|---|---|---|---|---|---|---|---|
| | | | | | | Kobe0065 | Kobe2602 | Sorafenib |
| SW480 | Colon | K-RasG12V | | | | 66.30 | 65.00 | 83.80 |
| PANC-1 | Pancreas | K-RasG12D | | | | 63.50 | 96.00 | 96.30 |
| EJ-1 | Bladder | H-RasG12V | | | | 62.70 | 51.50 | 87.70 |
| HT1080 | Connective tissue | N-RasQ61L | | | | 79.00 | 80.50 | 70.00 |
| DLD-1 | Colon | K-RasG13D | | | E545K | 60.50 | 63.00 | 80.70 |
| HCT116 | Colon | K-RasG13D | | | H1047R | 55.00 | 59.00 | 99.00 |
| A375 | Melanoma | | V600E | | | 26.00 | 41.00 | 93.00 |
| T-47D | Breast | | | | H1047R | 11.00 | 25.00 | 97.00 |
| LNCap | Prostate | | | frameshift | | 49.00 | 23.00 | 87.00 |
| BxPC-3 | Pancreas | | | | | 15.00 | 24.00 | 59.70 |
| MCF-7 | Breast | | | | E545K | 26.00 | 27.00 | 93.00 |
| HepG2 | Liver | | | | | 14.50 | 0.00 | 72.50 |
| HeLa | Cervix | | | | | 13.50 | 23.50 | 86.90 |

Experiments were performed three times, and each experiment used two wells per compound.

**Figure 1.5** Inhibitory effect of the Kobe0065-family compounds on anchorage-independent cell growth. (A) H-*rasG12V*-transformed (left) and c-*raf-1S259A/Y340D/Y341*-transformed (right) NIH3T3 cells were inoculated in the medium containing 10% FBS, 0.33% SeaPlaque agarose, and the indicated concentrations of the compound. After incubation at 37 °C for 14 days, the number of colonies with >200-μm diameter was counted. The values are presented as the mean ± SEM. * $P < 0.001$. (B) Effect of the 20 μM compounds on colony formation in soft agar of various human cancer cell lines. *Modified from Ref. [16].*

## 4.3. Inhibition of tumor growth in a xenograft model

The antitumor activities of the Kobe0065-family compounds were examined by using a xenograft of human colon carcinoma SW480 cells carrying the K-*rasG12V* gene grafted on athymic nude mice. Daily administration *per os* of Kobe0065 and Kobe2602 at the dose of 80 mg/kg for 18 days caused approximately 40–50% inhibition of the tumor growth. The activity of Kobe0065 became more evident at 160 mg/kg reaching about 60% inhibition, which was still a bit weaker than 65% inhibition attained by sorafenib at 80 mg/kg (Fig. 1.6A). During the compound treatment, the mice did not

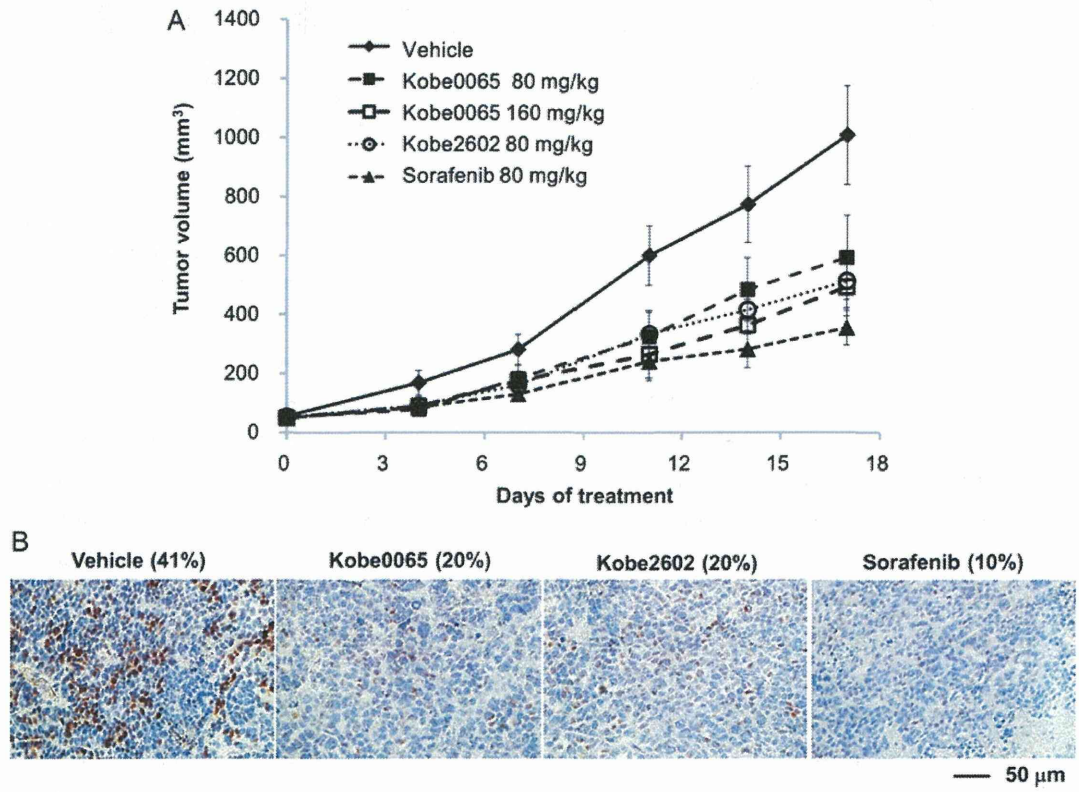


**Figure 1.6** Antiproliferative activity of the Kobe0065-family compounds on a tumor xenograft. (A) Female athymic nude mice were implanted with SW480 cells in their right flanks. When the tumor sizes reached $52 \pm 3$ mm$^3$, the compounds were administered orally for 5 consecutive days per week for 17–20 days at the indicated doses and the tumor volumes were continuously monitored. The values are presented as the mean $\pm$ SEM. $P = 0.086$ (*t*-test) for 80 mg/kg Kobe0065, $P < 0.05$ for 160 mg/kg Kobe0065 and 80 mg/kg Kobe2602, and $P < 0.01$ for 80 mg/kg sorafenib at day 17. One-way ANOVA with Tukey's test was used to analyze the significance of tumor size changes compared to the vehicle-treated group. (B) Phosphorylated ERK was detected by immunohistochemistry with an anti-pERK antibody in sections of tumors, which were treated daily with the 80 mg/kg compound for 17 days. The percentage of pERK-positive cells is shown on the top of each panel. *Modified from Ref. [16].*

exhibit any obvious abnormalities including weight loss. Immunostaining of the tumor sections with an anti-phosphoERK antibody showed that the ERK activation was substantially compromised by the compound administration (Fig. 1.6B). Moreover, tumors from the compound-treated mice showed a prominent increase of the apoptotic cell population, suggesting a contribution of the oncogene addiction mechanism to the antitumor effect of the compounds. Contrary to sorafenib, the Kobe0065-family compounds did not show the activity to inhibit tumor angiogenesis [16].

## 5. STRUCTURAL BASIS FOR INHIBITION OF Ras FUNCTIONS BY THE Kobe0065-FAMILY COMPOUNDS

Structural information on a Ras·GTP-compound complex is essential for not only the analysis of the inhibition mechanism but also the structural optimization of the compounds. We first attempted to crystallize the complex of the Kobe0065-family compound with H-RasT35S·GppNHp [10], which predominantly assumes state 1 conformation in solution and could be crystallized as state 1. To circumvent the low water solubility of Kobe0065 and Kobe2602, we added a water-soluble analogue named Kobe2601 (Fig. 1.7A), which showed weak inhibitory activity toward Ras–Raf binding with the $K_i$ value of $773 \pm 49$ μM to the list of compounds to be screened for cocrystallization with H-RasT35S·GppNHp. However, we failed to obtain crystals of sufficient quality to show the electron density of the compound by employing the cocrystallization or soaking method.

Failure in crystallization prompted us to use NMR spectroscopy to obtain structural information on the compound-binding interface on Ras·GTP. Again, we used H-RasT35S·GppNHp as a target because the NMR structure corresponding to state 1 had been determined for this mutant only [11]. This is because this mutation almost eliminated the slow conformational exchange process around the putative drug-binding pocket, which made NMR analysis of the wild-type protein impractical [11,21]. We used Kobe2601 for measurements of the nuclear Overhauser effects (NOEs), which need high concentration of the compounds in aqueous solutions. NOEs between the benzene rings of Kobe2601 and the side chains of H-RasT35S·GppNHp were detected and the collected data were used for calculation of the tertiary structure of the H-RasT35S·GppNHp-Kobe2601 complex (Fig. 1.7A). In the solved structure, the fluorobenzene ring of Kobe2601 was located in close proximity to the side chains of Lys5, Leu56, Met67, Gln70, and Tyr74 of H-Ras. These six residues formed a

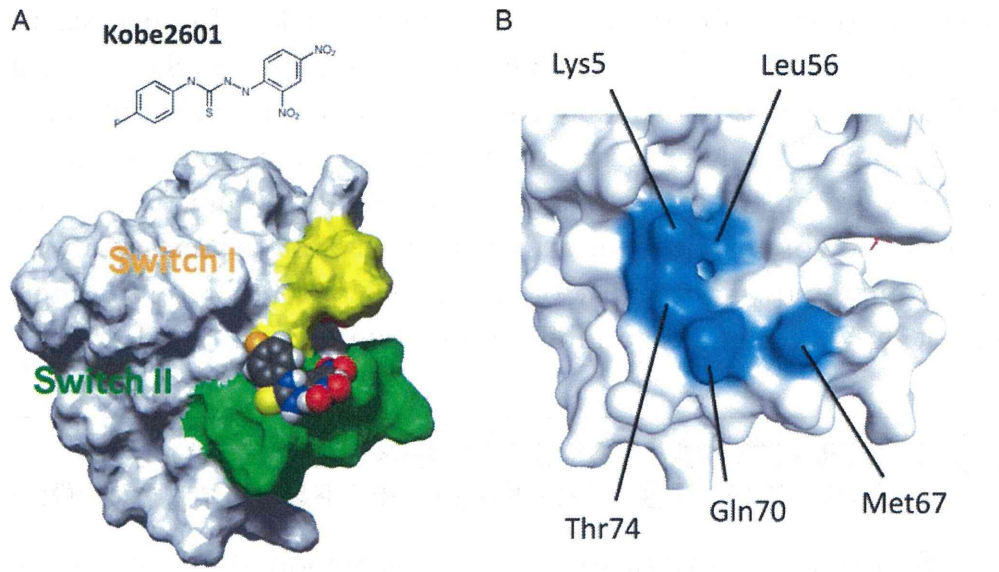


**Figure 1.7** Molecular basis for interaction of Ras·GTP with the Kobe0065-family compounds. (A) The lowest energy solution structure of the H-RasT35S·GppNHp–Kobe2601 complex. H-RasT35S·GppNHp is shown by a surface model (switch I, yellow; switch II, green) while Kobe2601 is shown by a space-filling model (C, black; O, red; N, blue; H, gray; S, yellow; F, orange). (B) A close-up view of the Kobe2601-binding pocket in the solution structure of H-RasT35S·GppNHp–Kobe2601 complex. Residues showing the intermolecular NOEs were highlighted in blue. *Panel (A): Reproduced from Ref. [16].*

hydrophobic surface pocket in the neighborhood of switch I (Fig. 1.7B) like the case with M-RasP40D·GppNHp, indicating that the fluorobenzene ring was inserted into the pocket through hydrophobic interaction. On the other hand, the dinitrobenzene moiety of Kobe2601 was located close to switch II in the model but did not appear to be tightly fixed to switch II (Fig. 1.7A). Although it was difficult to directly assign Kobe2601-interacting residues on wild-type H-Ras, measurement of the backbone amide $^{1}H$,$^{15}N$ heteronuclear single quantum coherence (HSQC) spectra of H-Ras·GppNHp revealed that the resonances from Leu56, Met67, and their neighboring residues underwent significant chemical shift changes and line broadening by the addition of Kobe2601 [16], suggesting that wild-type H-Ras shares a common drug-binding interface with H-RasT35S.

To analyze the molecular mechanism underlying the inhibition of Ras functions by the compounds, the NMR structure of the H-RasT35S·GppNHp-Kobe2601 complex was superimposed with the reported crystal structures of various Ras–effector complexes [22–24] (Fig. 1.8A–D). As for c-Raf-1 RBD [22], flurobenzene and nitrobenzene moieties of Kobe2601 were likely to cause steric hindrance with its surface

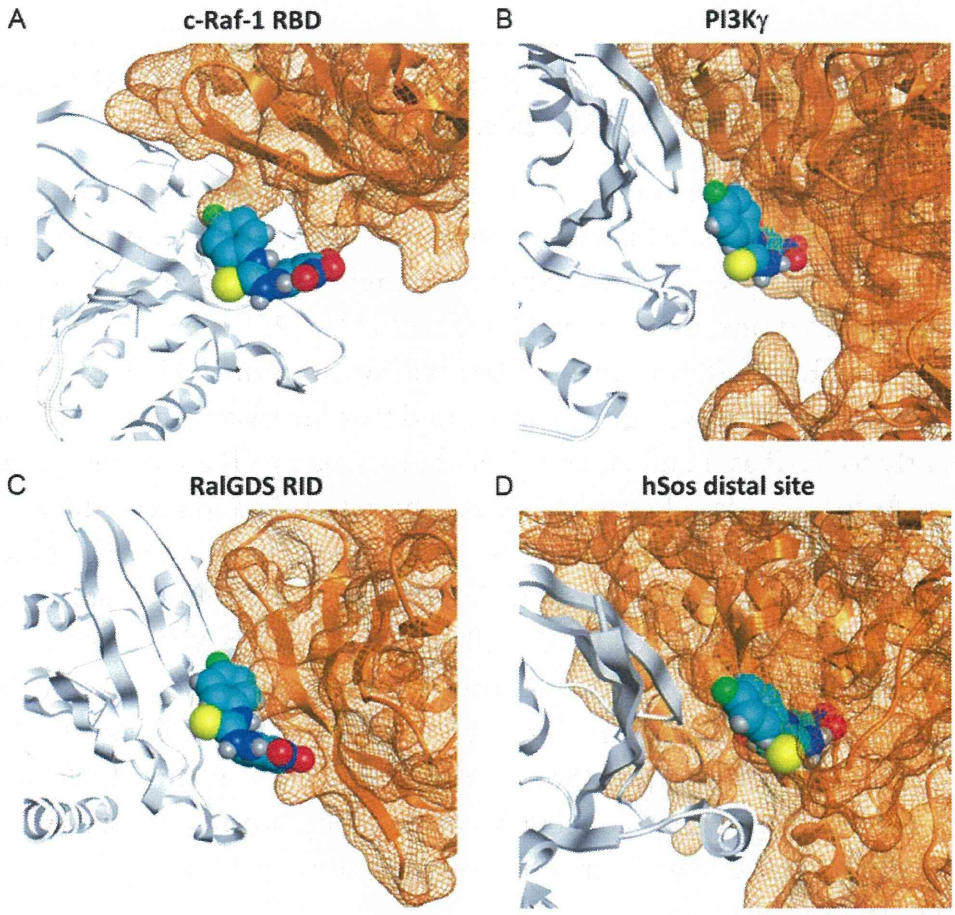


**Figure 1.8** Structural basis for inhibition of the Ras–effector interaction by the Kobe65-family compounds. The NMR structure of the H-RasT35S·GppNHp–Kobe2601 complex with the lowest energy target function was superimposed on the Ras or Rap1 molecule in the crystal structures of the Rap1A·GppNHp–c-Raf-1–RBD complex (PDB ID: 1C1Y) (A) H-RasG12V·GppNHp-PI3Kγ complex (PDB ID: 1H8E) (B) H-RasE31K·GppNHp–RalGDS–RID complex (PDB ID: 1LFD) (C) and H-RasY64A·GppNHp–hSos complex (PDB ID: 1NVV) (D) by fitting to minimize root mean square deviations for the residues 1–31, 39–59, and 76–166. H-RasT35S and the effectors are colored in white and brown, respectively. Kobe2601 is represented by a space-filling model. *Reproduced from Ref. [16].*

residues (Fig. 1.8A), supporting our observation of the competitive inhibition by Kobe0065 and Kobe2602. Further, a major part of Kobe2601, including the thiosemicarbazide and nitrobenzene moieties, was predicted to interfere with PI3K [23] much more heavily than with c-Raf-1 RBD (Fig. 1.8B), which may account for the inhibition of Akt phosphorylation by lower concentrations of Kobe0065 (Fig. 1.3D). Furthermore, Kobe2601 was predicted to interfere with the Ras-interacting domain (RID) of RalGDS [24] (Fig. 1.8C) and also more heavily with the distal site of hSos (19) (Fig. 1.8D), which were consistent with our results (Fig. 1.3E).

## 6. SPECIFICITY OF THE Kobe0065-FAMILY COMPOUNDS TOWARD VARIOUS SMALL GTPases

Since the residues constituting the compound-binding interface are well conserved among Ras-family small GTPases, the Kobe0065-family compounds were predicted to exhibit a rather broad specificity. By using relaxation-edited one-dimensional (1D) $^{1}$H NMR [25], we examined direct interaction of Kobe0065 and Kobe2602 with various small GTPases in their GppNHp-bound forms (Fig. 1.9) and found that the two compounds bound efficiently to M-Ras, Rap2A, and RalA but weakly to Rap1A compared to H-Ras. As for Rho-family small GTPases, both Cdc42 and Rac1 showed no detectable binding activity, while RhoA seemed to show some binding activity toward Kobe0065 but not Kobe2602. Also, we found that the compounds bound to H-Ras·GDP as well in the 1D $^{1}$H NMR analysis. This result was rather unexpected considering that the compounds failed to show any inhibitory effects on the intrinsic GEF catalytic activity of mSos1 (Fig. 1.3E). Further interpretation of the significance of this result on the action mechanism of the Kobe0065-family compounds will need further structural information on their actual binding sites on H-Ras·GDP, which is totally lacking at present.

## 7. DISCUSSION AND CONCLUSION

Since the middle 1990s, $^{31}$P NMR spectroscopic studies on Ras have unveiled their novel structural feature, that is conformational dynamics of their GTP-bound forms exhibiting equilibrium between two distinct conformational states, state 1 and state 2, which are characterized by different chemical shift values for the resonances of the nucleotide phosphorus atoms of the α-, β-, and γ-phosphate groups of bound GTP. [26]. Subsequent analyses have reached the conclusion that this conformational equilibrium is a general property shared by Ras-family members irrespective of the nature of the bound guanine nucleotide: GTP, GppNHp, or GTPγS [27–30]. However, the state distribution exhibits a great variation even among closely related GTPase species; the state 1 population occupies 36 ± 2%, 15 ± 1%, and 93 ± 2% for H-Ras, Rap1A, and M-Ras in complex with GppNHp, respectively [9,29], which possess the identical switch I residues and share some of the effectors such as c-Raf-1. Since the binding of Ras·GppNHp with its effectors induces a shift of the equilibrium toward state 2, state 1

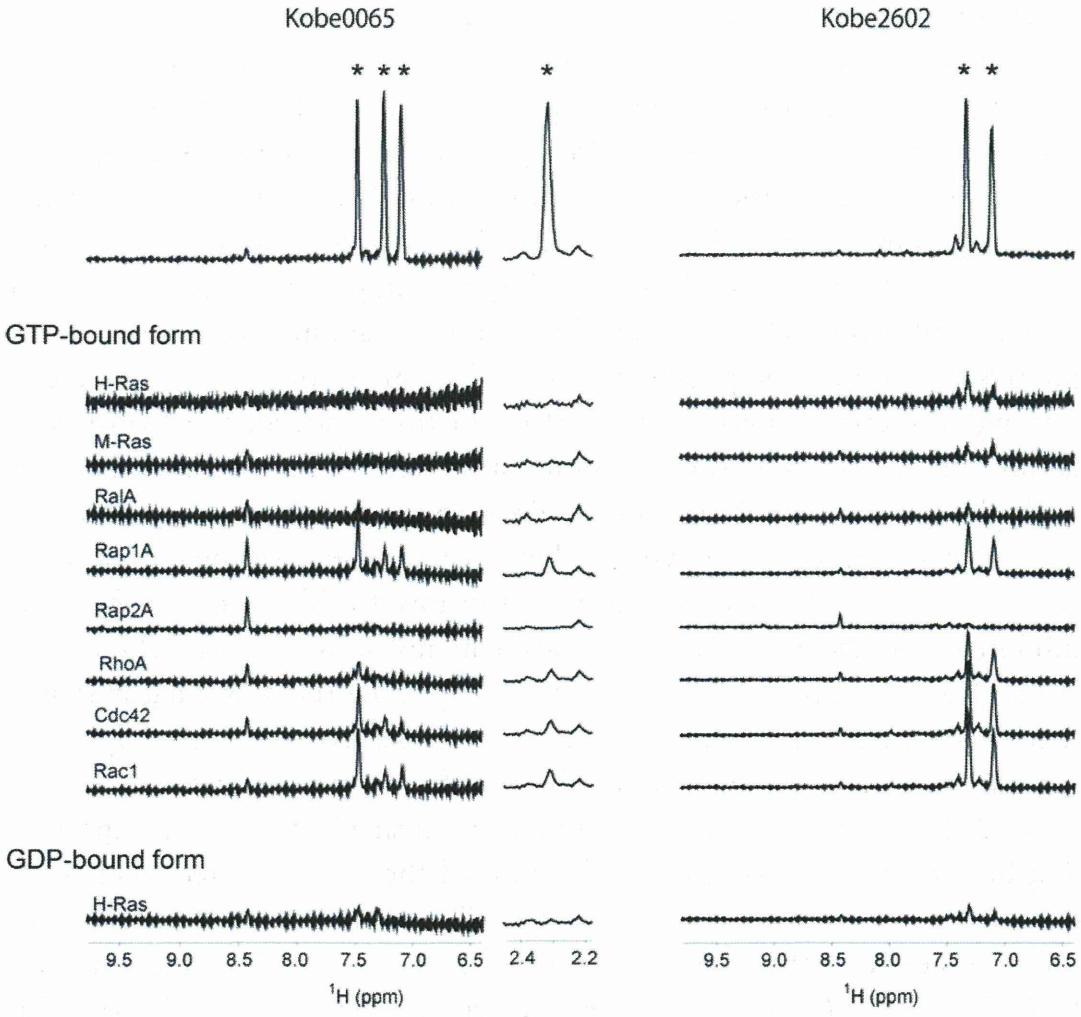


**Figure 1.9** Relaxation-edited 1D $^1$H NMR analysis of the interaction of the Kobe0065-family compounds with various small GTPases. Direct interaction of Kobe0065 and Kobe2602 with the indicated small GTPases was analyzed at a compound/protein molar ratio of 1:3 by relaxation-edited 1D NMR. All of the spectra were acquired with a CPMG spin-lock time of 400 ms. The compound specific signals in the spectra (top), indicated by asterisks, show line broadening and height reduction and eventually disappear when the compound binds directly to the small GTPases. The residual signal at 8.4 ppm was derived from an impurity in the sample buffer. *Reproduced from Ref. [16].*

and state 2 are presumed to represent inactive and active conformations, respectively. Crystal structures of H-Ras·GppNHp alone or in complex with the effectors all corresponded to state 2 [8,22–24]. By contrast, the existence of the state 1 conformation was indirectly evidenced by $^{31}$P NMR and electron paramagnetic resonance studies [26,31] until the first state 1 crystal structure of M-Ras·GppNHp was reported by our group in 2005 [9]. We further went on to investigate the molecular mechanisms for the state

transition through determination of a series of crystal structures corresponding to either state and their possible intermediates using M-Ras, H-Ras, and their mutants [9,10,12,32]. At the same time, these studies led to the discovery of "druggable surface pockets" as a common structural feature of the state 1 conformation, which was used for the *in silico* screening to identify the Kobe0065-family compounds as described in Sections 2 and 3. *In silico* screening targeting the surface pocket of M-RasP40D·GppNHp was initially conducted aiming to identify compounds that fit into the pocket and block its conversion to state 2, thereby causing allosteric inhibition of the Ras function. Indeed, the Kobe0065-family compounds were shown to inhibit the interaction of Ras·GTP with multiple effectors both *in vitro* and *in vivo* through insertion into the pocket. However, our recent $^{31}$P NMR studies have revealed that the compounds' activity to block the state transition is too low to fully account for their inhibitory activity of the Ras functions (data not shown). Thus, the mechanism of action of the Kobe0065-family compounds remains unclear at present; it seems to be ascribable to direct competitive inhibition by steric hindrance rather than allosteric inhibition of the state transition.

In 2012, Maurer *et al.* reported discovery of small-molecule compounds that bound to K-Ras4B·GDP and inhibited the Sos-mediated nucleotide exchange both *in vitro* and *in vivo* [33]. The crystal structure analyses of the complexes of the compounds, benzimidazole (BZIM), benzamidine (BZDN), and 4,6-dichloro-2-methy-3-aminoethyl-indole (DCAI), with K-Ras4B in complex with GDP and various GTP analogues, provided a molecular basis for inhibition of the Ras·GDP–Sos interaction but not the Ras·GTP/effector interaction. The compounds apparently interfered with the binding of K-Ras4B·GDP to Sos but not any effectors. Although the residues responsible for the interaction with BZDN and DCAI detected by the HSQC analysis overlapped partly with those identified by our NOE analysis with Kobe2601, a considerable difference exists in the location of the binding pockets and the orientation of the compounds [16], which seems to account for the difference in their ability to interfere with the effector interaction. Namely, the binding pocket for BZDN and DCAI in K-Ras4B·GTP is located close to Asp-54, whose side chain forms a direct hydrogen bond with the NH group of BZDN, whereas Kobe2601 is too far to establish any direct interactions with Asp-54. Sun *et al.* [34] also reported small-molecule inhibitors of K-Ras·GDP, which blocked the Sos-mediated nucleotide exchange *in vitro* and shared the binding pocket on Ras·GDP with BZIM, BZDN, and DCAI. Furthermore,

Hocker *et al.* [35] reported andrographolide derivatives that blocked guanine nucleotide exchange and inhibited the oncogenic Ras function although the binding site of the compounds on Ras·GDP was not determined. Thus, many researchers in diverse research fields such as pharmacology, structural biology, and molecular biology are currently focusing on the development of inhibitors targeting Ras·GDP to block its Sos-mediated nucleotide exchange. However, at present, it is not clear whether Sos inhibition is an effective strategy for suppressing the constitutively activated Ras mutants, considering the substantial reduction of their GTPase activity and a vast excess of free GTP over GDP in cellular concentrations. Although Sos inhibition might be effective for some cancer types considering that the function of wild-type Ras is required for the growth of tumors carrying the activated Ras [36], our results showing that the RasG12V·GTP level was almost unaffected by the cellular mSos1 level [16] indicate that H-RasG12V escapes from the upstream regulation by Sos. Finally, it must be mentioned that recent advances in discovery of Ras inhibitors targeting posttranslational modifications or plasma membrane recruitment are beyond the scope of this review.

In conclusion, we have discovered the Kobe0065-family compounds that bind to Ras·GTP and exhibit antiproliferative activity toward cancer cells carrying the activated *ras* oncogenes, by a novel strategy based on SBDD. The compounds efficiently inhibit the interaction of Ras·GTP with multiple effectors including Raf, PI3Ks, and RalGDS and a regulator/effector Sos, and show rather broad binding specificity toward various Ras-family members, which may account for their higher potency at the cellular level compared to that of the *in vitro* binding inhibition. Although the inhibitory activity is not particularly potent at present with the order of $10^{-6}$–$10^{-5}$ M, the Kobe0065 family compounds may serve as a lead scaffold for the development of Ras inhibitors with higher potency and specificity and low toxicity, which are suitable for clinical application. For this purpose, we would propose two possible strategies for structural optimization; the addition of a functional group, which gains a hydrogen-bonding or ionic interaction with the charged residues such as Asp-54 to increase the avidity, and the avoidance of the thiosemicarbazide structure, which is anticipated to lead to the cellular toxicity.

Finally, the discovery of novel Ras inhibitors reviewed in this chapter proves the effectiveness of our strategy of SBDD targeting Ras·GTP. After this study, we have conducted a large-scale *in silico* screen of a virtual library of over 2,000,000 compounds and successfully identified a couple of Ras

inhibitors whose basic structures are different from the Kobe0065-family showing more potent inhibitory activities both *in vitro* and *in vivo*. In the near future, such development process will be accelerated by further improvements in *in silico* screening methods and structure-based optimization strategies as well as refinement of the target structural model of Ras·GTP leading to generation of clinically useful Ras inhibitors.

## ACKNOWLEDGMENTS

This work was supported by the Program for Promotion of Fundamental Studies in Health Sciences of the National Institute of Biomedical Innovation (NIBIO) (to T. K.), Health and Labour Sciences Research Grant (to T. K.), JSPS KAKENHI Grant Nos. 20590280 and 23590336 (to F. S.), MEXT KAKENHI Grant Nos. 17014061 (to T. K.) and 18057014 (to F. S.), and MEXT Global COE Program A08 (to T. K.).

## REFERENCES

[1] A.E. Karnoub, R.A. Weinberg, Ras oncogenes: split personalities, Nat. Rev. Mol. Cell Biol. 9 (7) (2008) 517–531.
[2] I.R. Vetter, A. Wittinghofer, The guanine nucleotide-binding switch in three dimensions, Science 294 (5545) (2001) 1299–1304.
[3] B. Weinstein, Cancer. Addiction to oncogenes—the Achilles heal of cancer, Science 297 (5578) (2002) 63–64.
[4] L. Chin, et al., Essential role for oncogenic Ras in tumour maintenance, Nature 400 (6743) (1999) 468–472.
[5] K. Podsypanina, K. Politi, L.J. Beverly, H.E. Varmus, Oncogene cooperation in tumor maintenance and tumor recurrence in mouse mammary tumors induced by Myc and mutant Kras, Proc. Natl. Acad. Sci. U.S.A. 105 (13) (2008) 5242–5247.
[6] G.L. James, J.L. Goldstein, M.S. Brown, Polylysine and CVIM sequences of K-RasB dictate specificity of prenylation and confer resistance to benzodiazepine peptidomimetic in vitro, J. Biol. Chem. 270 (11) (1995) 6221–6226.
[7] B. Rotblat, M. Ehrlich, R. Haklai, Y. Kloog, The Ras inhibitor farnesylthiosalicylic acid (Salirasib) disrupts the spatiotemporal localization of active Ras: a potential treatment for cancer, Methods Enzymol. 439 (2008) 467–489.
[8] E.F. Pai, et al., Structure of the guanine-nucleotide-binding domain of the Ha-ras oncogene product p21 in the triphosphate conformation, Nature 341 (6239) (1989) 209–214.
[9] M. Ye, et al., Crystal structure of M-Ras reveals a GTP-bound "off" state conformation of Ras family small GTPases, J. Biol. Chem. 280 (35) (2005) 31267–31275.
[10] F. Shima, et al., Structural basis for conformational dynamics of GTP-bound Ras protein, J. Biol. Chem. 285 (29) (2010) 22696–22705.
[11] M. Araki, et al., Solution structure of the state 1 conformer of GTP-bound H-Ras protein and distinct dynamic properties between the state 1 and state 2 conformers, J. Biol. Chem. 286 (45) (2011) 39644–39653.
[12] S. Muraoka, et al., Crystal structures of the state 1 conformations of the GTP-bound H-Ras protein and its oncogenic G12V and Q61L mutants, FEBS Lett. 586 (12) (2012) 1715–1718.
[13] D. Sitkoff, K.A. Sharp, B. Honig, Accurate calculation of hydration free energies using macroscopic solvent models, J. Phys. Chem. 98 (7) (1994) 1978–1988.